Project Title: Transport properties of self-propelled micro-swimmers

Name: Franco Nori (1,2), Vyacheslav R. Misko(1), and Pulak Kumar Ghosh (1,3)

(1) Theoretical Quantum Physics Laboratory, RIKEN Cluster for Pioneering Research, Wako-shi, Saitama 351-0198, Japan

(2) Department of Physics, University of Michigan, Ann Arbor, Michigan 48109-1040, USA

(3) Department of Chemistry, Presidency University, 86/1 College Street, Kolkata 700073, India.

Laboratory at RIKEN:

Theoretical Quantum Physics Laboratory, RIKEN Cluster for Pioneering Research, Wako-shi, Saitama 351-0198, Japan

1. Background and purpose of the project, relationship of the project with other projects

The diffusion of a tracer (organic or artificial, alike) in a suspension fluid is a standard problem of classical transport theory. Combination of two distinct aspects of this phenomenon, which recently attracted widespread interdisciplinary interest, each for its own merit: (i) the persistent (or time-correlated) random motion of self-propelling particles and (ii) colloidal dispersion in laminar flows.

The most tractable example of persistent Brownian motion is represented by artificial micro-swimmers, namely tiny Brownian particles capable of self-propulsion in an active medium [ref]. Such particles are designed to harvest environmental energy by converting it into kinetic energy. A class of artificial swimmers widely investigated in the current literature is the so-called Janus particles (JP), mostly spherical colloidal particles with two differently coated hemispheres, or ``faces". Recently, artificial micro- and nano-swimmers of this class have been the focus of pharmaceutical (e.g., smart drug delivery [1]) and medical research (e.g., robotic microsurgery ref.[2]).

These peculiar Brownian particles change direction randomly as usual, but with finite time scale; persistence makes their diffusion extremely sensitive to geometric confinement and other constraints.

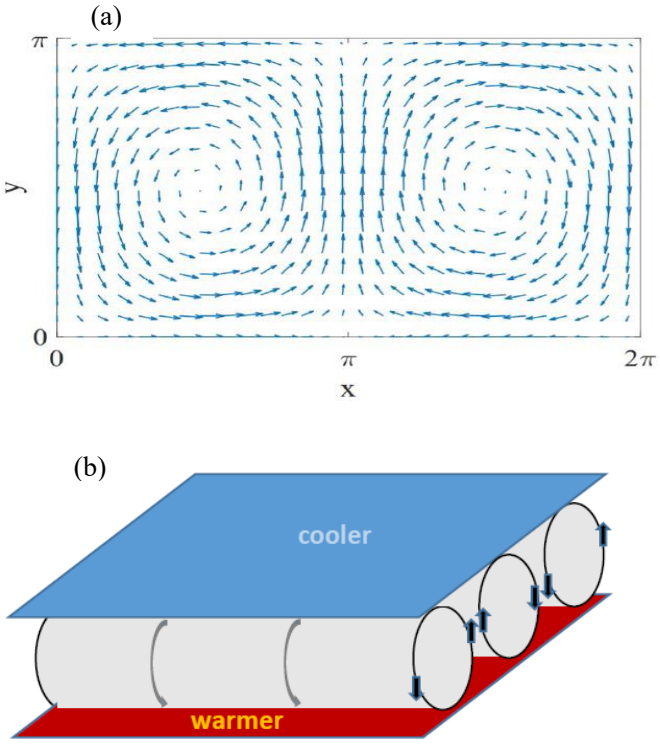

Fig.1: (a) Schematic for in the laminar flow of Eq.(1), and (b) set up for convection rolls produced due to temperature difference between top and bottom boundaries.

Technological applications involving sub-millimeter artificial swimmers thus require accurate control of their diffusive properties in non-homogeneous environments.

On the other hand, Brownian diffusion in an advective medium is also nanotechnological issue, for instance, in the design and operation of microfuidic devices or chemical reactors. Let us consider a Brownian tracer of free diffusion constant D_0, advected by the free-boundary stationary laminar flow with stream function,

$$\psi(x,y) = \frac{U_0 L}{2\pi} \sin\left(\frac{2\pi x}{L}\right) \sin\left(\frac{2\pi y}{L}\right) \quad - - (1)$$

At high Peclet numbers, $Pe = D_L/D_0 >> 1$, a passive tracer undergoes normal diffusion with enhanced diffusion constant, $D = k(D_L D_0)^{1/2}$ with k = 1.065, that is $D > D_0$. This advection effect, termed advection enhanced diffusivity (AED), has been explained by noticing that for $D_0 < D_L$ an unbiased particle jumps between convection rolls while being advected along their separatrices. Narrow flow boundary layers (FBL) of estimated width $\delta = (D_0/\Omega_L)^{1/2}$, form a network of advection channels centered around the ψ(x,y) cell separatrices, thus enabling a large-scale particle's diffusion.

Peculiar effects due to the combination of self-propulsion and advection are expected to emerge when one considers an active JP suspended in a one dimensional (1D) array of counter-rotating convection rolls. An ideal experimental setup is sketched in Fig.1 (b). An array of stationary Rayleigh-Benard cells can occur in a plane horizontal layer of fluid heated from below. Assuming that they are counter-rotating cylinders parallel to the z-axis, the z coordinate of a suspended tracer is ignorable; hence the reduced two dimensional (2D) flow pattern of Eq.(1). Advection enhanced diffusivity of passive colloidal particles in arrays of Rayleigh-Benard rolls has already been demonstrated experimentally. Experimental data on the dispersion of self-propelling microswimmers in convective laminar flows are scarce. In this regard, active JPs are ideal tracers for this kind of measurements because self-propulsion speed can be conveniently tuned with respect to the advection drag established in the convection cell.

2. Specific usage status of the system -- This fiscal year we mainly used Hokusai supercomputer mainly for the above mentioned project and produced some interesting results presented in the next section. However, to complete this project more simulation need to be done. In addition to this item, we used super computer for some calculation related to diffusion in binary mixture of self-propelled Janus particle [5].

3. Theoretical and simulation method

Model - By (linear) convection array we mean here a stationary laminar flow with periodic stream function like ψ(x,y) of Eq.(1), confined between two parallel edges, y = 0 and y = L/2, which act as dynamical reflecting boundaries. The unit cell of the array consists of two counter-rotating convection rolls [Fig.2(a)]. The dynamics of an overdamped active JP can then be formulated by means of two translational and one rotational Langevin equation (LE),

$$\begin{aligned} \dot{\mathbf{r}} &= \mathbf{v}_\psi + \mathbf{v}_0 + \sqrt{D_0}\,\boldsymbol{\xi}(t) \\ \dot{\theta} &= (\alpha/2)\,\nabla \times \mathbf{v}_\psi + \sqrt{D_\theta}\,\xi_\theta(t \end{aligned} \quad - - (2)$$

where r = (x,y), $\mathbf{v}_\psi$ and $\mathbf{v}_0$ are advection and self-propelled velocity respectively. The self-propulsion is oriented at an angle θ with respect to the longitudinal x-axis.

The translational (thermal) noises in the x- and y-directions,: $\xi_x(t)$, $\xi_x(t)$ and the rotational noise,$\xi_\theta(t)$, are stationary, independent, delta-correlated Gaussian noises, .

$$\left\langle \xi_i^q(t) \right\rangle = 0$$
$$\left\langle \xi_i^q(t)\xi_j^{q'}(0) \right\rangle = 2\delta_{ij}\delta_{qq'}\delta(t)$$

Where q or q' = {*x, y, θ*}. D_0 and D_θ are the respective noise strengths, which for generality we assume to be unrelated. To avoid uncontrolled hydrodynamic effects, the particle is taken to be point like. Other effects due to its actual geometry and chemical-physical characteristics are encoded in the model dynamical parameters. The reciprocal of D_θ coincides with the angular persistence (or correlation) time. The flow shear exerts a torque on the particle proportional to the local fluid vorticity. For simplicity, we adopt second law, which, for an ideal no-stick spherical particle, yields.

Simulation method - We numerically integrated Eqs. (1-3) using a standard Milstein algorithm to obtain diffusivity, mobility and probability density function. The numerical integration was performed using a very short time step, 10^{-3} -10^{-4} to ensure numerical stability. At t = 0, the particles were uniformly distributed in cell of convection roll with random orientation. The data points reported in the figures shown here,have been obtained by ensemble averaging over a minimum of 10,000 trajectories. Particular caution was exerted when computing the asymptotic diffusion constant,

$$D = \lim_{t\hat{a}\dagger'\hat{a}\check{z}} \frac{< [x(t) - x(0)]^2 >}{2t}$$

and mobility,

$$\hat{I}¼ = \frac{< [x(t) - x(0)] >}{Ft}$$

Because for low values of the noise strengths, D_0 and D_θ, the transients of the diffusion process grow exceedingly long. For asymptotically large running times, our estimates of mobility, diffusivity and probability density functions are independent of the starting point (x(0),y(0)).

4. Results

Active particle diffusion in convection roll array

In sharp contrast with the noiseless limits the spatial distribution of a noisy active JP is not uniform. The outcome of our numerical simulations is summarized in Fig 2 and Fig3.

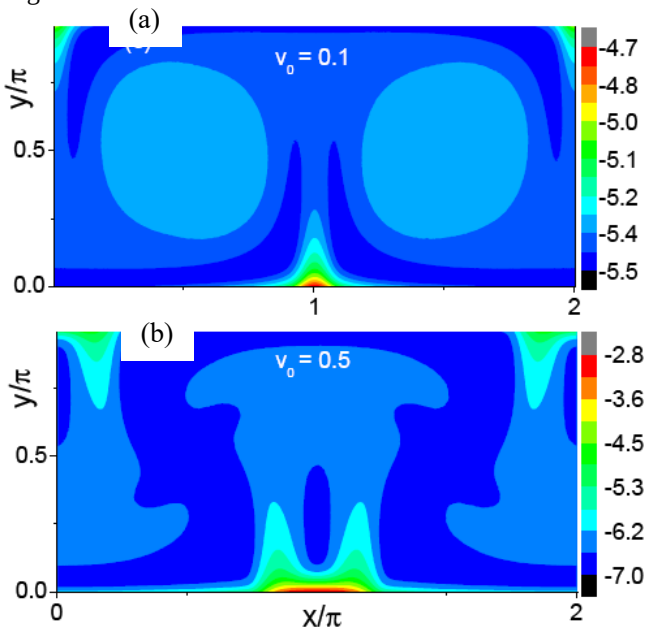

Fig.2: Stationary probability distribution in the convection cells for v_0=0.1 (a) and 0.5 (b). The chart levels are color-coded on natural logarithmic scales as indicated. Other simulation parameters are: D_0=0.01, D_θ = 0.01, U_0 = 1 and L = 2π.

The laminar flow acts upon the particle through both an advection drag and an advection torque. Along the roll boundaries the drag is maximum (with speed approaching U_0, except at the ``stagnation" corners), but the torque vanishes. At low self-propulsion speeds, this favours the orientation of v_0 parallel to the advection velocity v_ψ. The JP thus undergoes a large-scale intra-roll circulation motion, which causes its accumulation along the outer layers of the rolls. The less pronounced particle accumulation at the roll centers is attributable to the higher vorticity there. These two areas of accumulation are separated by a circular depletion

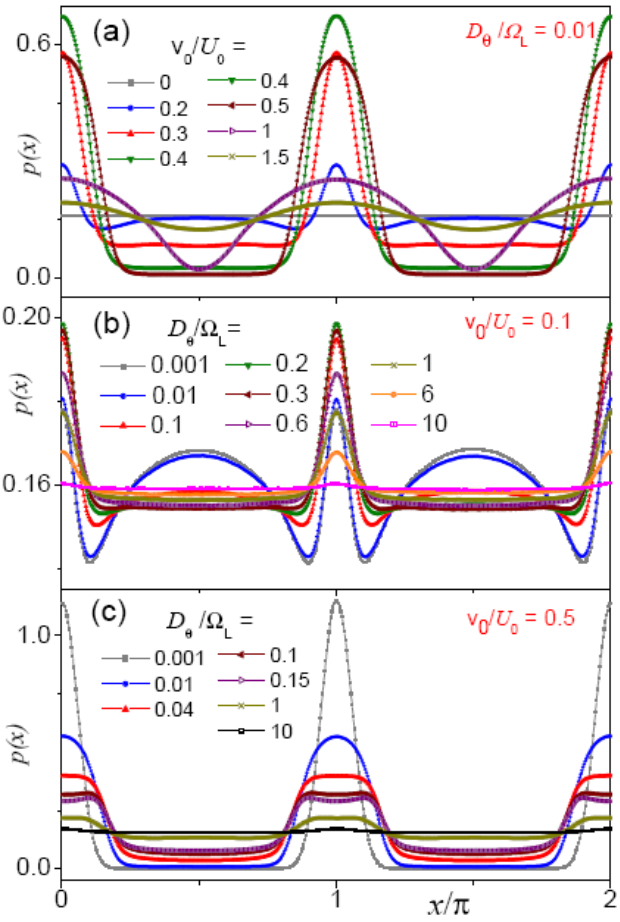

Figure 3: Stationary longitudinal distributions, p(x), of a JP in the laminar flow of Eq. (1) for (a) D_q = 0.01 and different v_0; (b) v_0 = 0.1 and (c) v_0 = 0.5 and different D_q (see legends). Other simulation parameters are: D_0 = 0.01; U_0 = 1 and L = 2π.

region. Indeed, in Fig 2(a) and Figs3.(a),(b) ref[6] the particle appears to be sucked in by the ascending (x = L/2) and descending boundary flows (x= 0, L) an effect that seems to increase with increasing v_0. This picture changes abruptly as v_0 is raised above a critical value v_c, which we established to depend on the strength of the thermal noise, D_0. The intra-roll circulation of Fig.2(a) is suppressed and the roll interior gets depleted [Fig.3(a),(b)]; as a result, the particle piles up symmetrically at the base of the ascending (bottom edge) and descending flows (top edges). Moreover, for $v_0 \geq U_0$, the particle seems to diffuse mostly along the array's edges, which explains why the longitudinal distributions, p(x), turn uniform again with increasing v_0, while the transverse distributions, p(y), remain peaked at y = 0, L/2. One also notices that the peaks of p(x) widen with increasing v_0 [Fig.3(a)] and D_θ [Fig.3(c)].

The relevance of these results can be best appreciated by comparison with the diffusion of a passive particle in the same 1D convection array. In that case, the flow boundary layers still control the particle's large-scale diffusion, but all stationary distributions, p(x, y), remain uniform. This conclusion applies also to noiseless self-propelling JPs in 1D convection arrays, as proven in Ref.[3], but is no longer true in the presence of thermal noise. Indeed, upon hitting either array edge, the particle will persist pointing against it for a time τ_θ; hence the angular correlation of $\mathbf{v}_0$ and $\mathbf{v}_\psi$. [Note that in most simulations presented here τ_θ is larger than the circulation characteristic time, i.e, $D_\theta < \Omega_L$]. Accordingly, no probability density accumulation at the roll boundaries was detected for an active JP in the 2D laminar flow of Eq.(1) with periodic boundary conditions, regardless of the noise strengths, D_0 and D_θ. This leads to the conclusion that the FBL structure we detected in the stationary distributions p(x, y) of an active JP diffusing in a 1D convection array is a combined effect of noise and geometric confinement.

The self-propulsion threshold, v_c, can be estimated as follows. When the vector $\mathbf{v}_0$ points inwards, the particle pulls away from the edge a length of the order of $v_0/4\Omega_L$, before being swept into a vertical flow layer. As such length grows comparable with the width of an unbiased flow boundary layers, i.e., for $v0 > v_c$ with

$$v_c / U_0 = 4\sqrt{D_0 / D_L}$$

the particle exits the FBL and its circulation along the roll separatrices is interrupted. This estimate of v_c is consistent with our simulation data for p(x) and p(y) at low angular noise,$D_\theta << \Omega_L$ [compare Figs. 2-3 see ref[ms] details]. Note, for instance, that in Fig.3 the p(x) regions delimited by the peaks at x=0, π and 2π get depleted only for $v_0 = 0.5$, that is for $v_0 > v_c$. Moreover, being confined in a FBL, a JP with $v_0 < v_c$ ought to behave like a passive colloidal particle, i.e, undergo advection enhanced diffusivity as an effect of the sole thermal noise. The diffusion data presented in the next section (Fig.~4) confirm this conclusion.

As the FBL circulation breaks up, the JP tends to accumulate against the array edges, provided that the self-propulsion length is larger than the array width, $l_\theta > L/2$. However, its motion along the edges is not advection-free. The coordinate x in Langevin equation obeys the approximate equation like:

$$\dot{x} = U_0 \left\langle \cos\left(\frac{2\pi y}{L}\right)\right\rangle \sin\left(\frac{2\pi x}{L}\right) + v_0 \cos\theta + \xi_x(t)$$

which describes the dynamics of a Brownian particle pinned to a washboard potential (advection term) and subjected to a colored, non-Gaussian tilting noise, $v_0 \cos\theta(t)$, with correlation time (self-propulsion term). The average $\langle\cos(2\pi y/L)\rangle$ depends on all three free parameters v_0, D_θ and D_0; in particular, its modulus increases with increasing v_0 and decreasing D_θ. This simple observation explains: (i) the non-monotonic v_0-dependence of the p(x) peaks, whereby a larger v_0 implies not only higher washboard potential barriers, but also a stronger tilting term; (ii) the flattening of the longitudinal distributions for $v_0 \geq U_0$, as self-propulsion wins over the advection pinning action at the edges; (iii) the broadening and double-peaked profile of the p(x) peaks in Fig.3(c) on increasing D_θ which is a well-known effect of colored noise.

On increasing D_θ, the JP self-propulsion length eventually grows shorter than the roll size, $l_\theta < L/2$; the active particle then tends to behave like a passive Brownian particle, except its free diffusion constant, D_0, must be now incremented by the extra term $D_s = v_0^2/2D_\theta$. Accordingly, both its spatial distributions, p(x) and p(y), become uniform [see Figs. 3(b),(c)].

Anisotropic exclusion effect between Ag/AgCl Janus particles and passive beads in a dense colloidal matrix

We studied the anisotropy in the interaction of visible light-driven Ag/AgCl-based spherical Janus particles embedded in a dense matrix of passive SiO2 beads in pure water (Figure 4). In contrast to prior works, 6 we considered the case when Janus particles are fixed to a glass substrate. Therefore, we primarily track the dynamic properties of the surrounding passive beads. We observe an anisotropic profile of the repulsive interaction between active Janus particles and passive beads and explain it as a result of an asymmetry in the chemical gradient around the Janus particle, triggered upon visible light illumination. This leads to the distortion in the initially isotropic surrounding electric potential and results in the asymmetric exclusion of passive beads around the Ag/AgCl cap. We follow the time evolution of a spatial distribution of passive beads and analyze their displacement around the Janus particle. We describe two limiting cases, when a Janus particle is completely immobile or it can perform rotational but no translational motion. With this study, we provide new insights into the rotational dynamics of photocatalytically active Janus particles embedded in a dense matrix of passive beads. We anticipate that these phenomena, peculiar for electro-kinetic motors, can be observed only due to the confinement imposed by a dense environment.

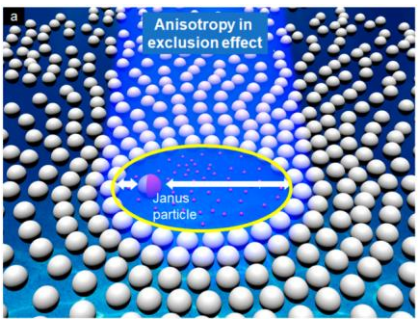

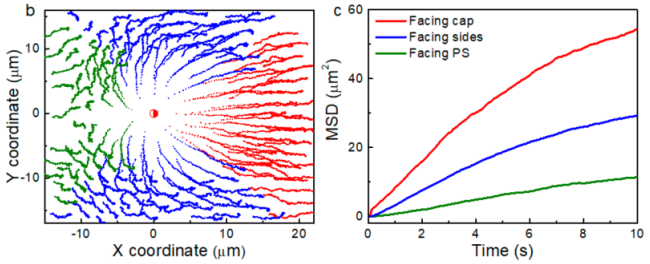

Figure 4. (a) Schematics of the asymmetry in the particle-bead repulsion in a soft matter system containing an immobilized active Janus particle in a dense matrix of passive beads. (b, c) Theoretical study of the interaction in a system containing an immobile Janus particle and passive beads. (b) Trajectories of passive beads. (c) MSD curves.

Inverse solidification induced by Janus particles

Macroscopic properties of solids are determined by their crystalline structure and its purity. Introducing defects in the lattice, by doping or increasing the temperature, results in the displacement of atoms of the initial crystal from their equilibrium positions. When these displacements exceed some critical value, the crystal melts turning to a liquid (Fig. 4a). Typically, defect-induced solid melting occurs via defect proliferation along the crystal-lattice directions, leading to the increase of the density of defects.

We demonstrated – in experiments and in numerical simulations [8] – a striking counter-intuitive behavior: the occurrence of long-range order in an initially disordered suspension of colloidal particles (Figs 4b, c). The observed ordering is induced by active defects, namely catalytic Janus particles, dispersed in a passive matrix of colloidal beads. Crystallization in the colloidal suspension is observed when the concentration of active defects increases and reaches a critical value. This situation is opposite to the classical defect-induced crystal melting observed in condensed and soft matter systems. This allows us to refer to the observed active-defect-induced solidification as to an inverse liquid-to-solid transition under increasing fluctuations.

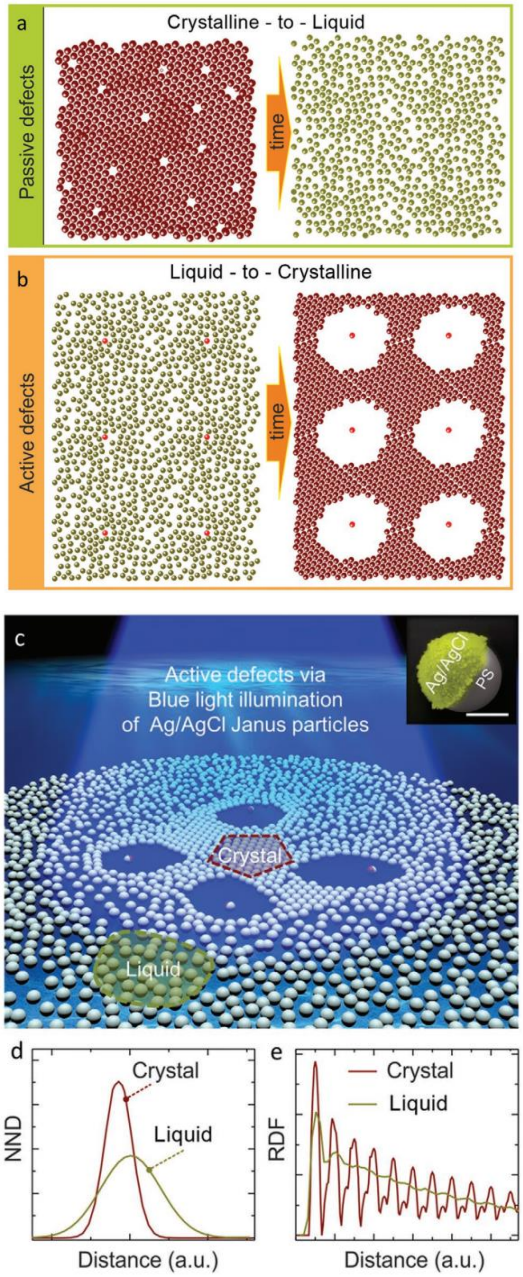

Figure 5. Concept of the liquid-to-crystalline phase transition due to internal drive. (a) Sketch illustrating a conventional defect-induced solid melting: a transition from crystalline to liquid state. (b) Liquid-to-crystalline transition induced by active defects. (c) Schematics of the experimental realization of the liquid-to-crystalline transition using a soft matter colloidal system. Inset in c: scanning electron microscopy (SEM) image of polystyrene (PS) based Janus particle where the Ag/AgCl cap is shown with false color. Scale bar, 1 μm. (d) Nearest neighbor distribution (NND) function for liquid and crystalline states. (e) Radial distribution function (RDF) showing one peak followed by a featureless tail if the system is in the liquid state. RDF with many sharp peaks is typical for a crystalline state.

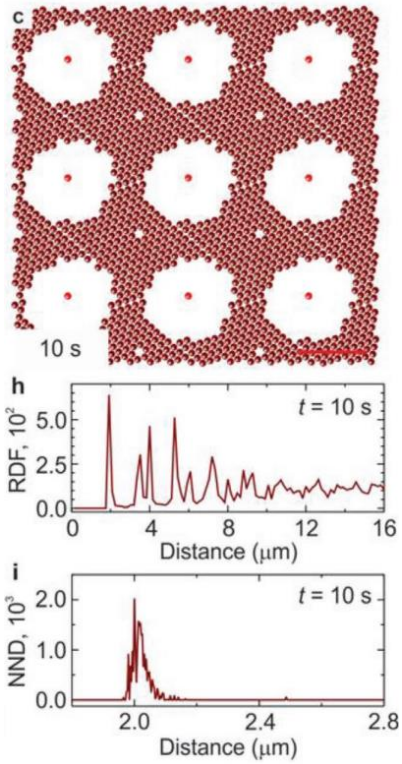

Figure 6. Emergence of a global crystalline state from an amorphous matrix due to internal drive (simulation). Scale bar, 20 μm. (c) Formation of a crystalline solid at t = 10 s: The corresponding RDF (h) shows many sharp peaks, and the NND (i) is represented by a narrow peak.

5. Conclusions

Active particle diffusion in convection roll array

We have investigated the diffusion of an active JP in a 1D array of counter-rotating convection rolls [6]. The JP considered here should be regarded as modeling a self-propelling micro-swimmer of biological or synthetic nature, alike. Our choice for the laminar flow is meant to mimic the Rayleigh-Benard rolls occurring between two parallel surfaces kept at an appropriate temperature difference.

We focused on effects due the combination of three key ingredients, namely, thermal noise, advection and self-propulsion, in a confined geometry. Such effects, not

detectable in 2D arrays of convection rolls with same hydrodynamical parameters but no boundaries, can be summarized as follows:

(i) The large-scale circulation of a JP trapped in a convection roll is confined to narrow flow boundary layers, whereby the particle self-propulsion velocity tends to line up with the advection drag, which results in an accumulation of the particle probability density.

(ii) The diffusion of an active JP with low self-propulsion speed is governed by its circulation along the roll boundaries, and is thus undistinguishable from that of a regular passive particle.

(iii) For larger self-propulsion speeds, the JP tends to sojourn in the vicinity of the array's edges and diffuses by sliding along them. Its diffusion is dominated by the advection drag parallel to the array's boundaries even for self-propulsion speeds much larger than the advection drag. This mechanism works for strengths of the angular noise above a certain threshold; below that threshold, the particle's diffusion constant drops to vanishingly small values.

Anisotropic exclusion effect between Ag/AgCl Janus particles and passive beads in a dense colloidal matrix

Synthetic nano- and micromotors interact with each other and their surroundings in a complex manner. We studied [7] the anisotropy of the active-passive particles interaction in a soft matter system containing a photochemical Ag/AgCl-based Janus particle embedded in a dense matrix of passive beads in pure water. The asymmetry in the chemical gradient around the Janus particle, triggered upon visible light illumination, distorts the isotropy of the surrounding electric potential and results in the repulsion of adjacent passive beads away from the Janus particle. Our study provides not only a novel fundamental insight into the collective behavior of a complex mixture of active and passive particles, but is also relevant for various applications, e.g., particles transport at micro- and nanoscale and local chemical sensing.

Inverse solidification induced by Janus particles

Crystals melt when thermal excitations or the defect concentration in the lattice is sufficiently high. In contrast to this classical scenario of solid melting, we demonstrated [8], in numerical simulations and in experiment, a counter-intuitive behavior: the occurrence of crystalline long-range order in an initially disordered matrix. This unusual solidification is realized in a system of passive colloidal particles accommodating active defects – photocatalytic Janus particles. The observed crystallization occurs when the amount of active-defect-induced fluctuations (which is the measure of the effective temperature) reaches critical value. The driving mechanism behind this unusual behavior is purely internal and resembles a blast-induced solidification. In our case, the role of "micro-blasts" is played by the chemically active Janus particles. The observed behavior can also be interpreted as an active-matter realization of the "freezing-by-heating" transition. The study of amorphous-to-crystalline phase transitions provides a novel insight into the collective effects in mixed colloidal systems of active and passive species. It offers versatile possibilities to address the processes of solidification in various systems brought out of equilibrium, including the formation of biomolecular condensates or biomineralization, transitions from amorphous to polycrystalline state in condensed matter, or the synthesis of materials under extreme conditions. The proposed inverse crystallization and reentrant mechanisms allow tailoring mechanical properties of new functional materials.

***

In addition to the research works described above, we are still working on other issues from last year’s in particular diffusion in binary mixture.

6. Future plan

In the next fiscal year, we plan to explore the following issues:

(i) **Diffusion of active particle in biased convection array**

We plan to extend our study of diffusion of active particle in convection array to analyze external bias like gravitation force. Our recent study on the transport of a biased passive colloidal particle in a one dimensional periodic array of planar counter-rotating convection rolls at high Peclet numbers produced very interesting results. It shows that advection enhanced diffusion is drastically suppressed by an external transverse bias, but strongly reinforced by a longitudinal drive of appropriate intensity. Both effects

occur independently of the imposed boundary conditions. The bias dependence of the diffusion constant is interpreted as a measure of the fluid-mechanical stability of the flow boundary layers governing diffusion in convection rolls.

This fascinating results motivate us to explore transport features of self-propelled particles in biased convection array. Dynamics of such particle can be described by a similar type of Langevin equation as Eq(2). However, here particle will encounter addition bias (F_x, F_y). The time evolution of the particles center of mass and direction of self-propulsion can be described as,

$$\dot{x} = u_x + v_0 \cos\theta + F_x + \xi_x(t),$$

$$\dot{y} = u_y + v_0 \sin\theta + F_y + \xi_y(t),$$

$$\dot{\theta} = \xi_y(t),$$

All the terms in the above equations have same meaning as in the precious section. Based on the numerical method describe in section we want to numerically solve this coupled differential equation to get diffusivity and mobility, the main transport quantifiers. However, to greater understand the underlying transport mechanism, details of particle trajectories as well as stationary distribution in the convection roll will be analysand for various parameter regimes.

(ii) Response of active Brownian particles to external drive in 2D square convection array.

Our preliminary studies show that response of an overdamped Brownian particle driven-advected in a 2D square convection array shows large deviations from the predictions of the linear response theory. While the mobility is independent of the drive orientation, its diffusion turns out to be strongly anisotropic. Depending on the drive orientation, the diffusion constants along the main array's axes exhibit distinct peaks for advection and external drags of comparable magnitude.

As a natural extension of the approach presented in this paper, we plan to investigate next the anisotropic response of active Brownian particles, either biological or synthetic, in convection arrays. We are confident that a better understanding of the diffusion of self-propelling particles in patterned convection flows is likely to play an important role in controlling driven transport of active matter in microfluidic devices.

To address the above-mentioned issues we will exploit the numerical scheme mentioned in Sec. III.

Currently, I have a "Quick Use" user account and I would like to get extension of computation facilities for next usage term (up to 31st March 2022) under the same user category.

References:

[1] Smart Drug Delivery System , edited by A. D. Sezer (IntechOpen, 2016). DOI: 10.5772/60475

[2] J. Wang, Nanomachines: Fundamentals and Applications, (Wiley-VCH, Weinheim, 2013).

[3] C. Torney and Z. Neufeld, Transport and aggregation of self-propelled particles in fluid flows, Phys. Rev. Lett. 99, 078101 (2007)

[3] P. K. Ghosh, V. R. Misko, F. Marchesoni, and F. Nori, Self-propelled Janus particles in a ratchet: Numerical simulations, Phys. Rev. Lett. 110, 268301 (2013).

[5] D. Debnath, P. K. Ghosh, V. R. Misko, Y. Li, F. Marchesoni and F. Nori, Enhanced motility in a binary mixture of active nano/microswimmers, Nanoscale 12, 9717 (2020).

[6] P. K. Ghosh, F. Marchesoni, Y. Li, and F. Nori, Active particle diffusion in convection roll array, manuscript under preparation 2021.

[7] Tao Huang, S. Gobeil, Xu Wang, V. Misko, F. Nori, W. De Malsche, J. Fassbender, D. Makarov, G. Cuniberti, and L. Baraban, Anisotropic Exclusion Effect between Photocatalytic Ag/AgCl Janus Particles and Passive Beads in a Dense Colloidal

Matrix, Langmuir 36, 7091−7099 (2020). Also featured as: Cover page of the Special Issue "Advances in Active Materials", Langmuir 36, issue 25 (2020).

[8] Tao Huang, V. R. Misko, S. Gobeil, Xu Wang, F. Nori, J. Schütt, J. Fassbender, G. Cuniberti, D. Makarov, L. Baraban, Inverse Solidification Induced by Active Janus Particles, Adv. Funct. Mater. 2003851 (2020). Also featured as: AFM Inside Front Cover: DOI:10.1002/adfm.202070260.

Fiscal Year 2020 List of Publications Resulting from the Use of the supercomputer

D. Debnath, P. K Ghosh, V. R Misko, Y. Li, F Marchesoni, F Nori,
Enhanced motility in a binary mixture of active nano/microswimmers,
Nanoscale volume - 12, issue 17, pages 9717-9726, 31st March 2020
(online publication date) DOI: 10.1039/d0nr01765e.

[Paper accepted by a journal]

None

[Conference Proceedings]

None

[Oral presentation]

None

[Poster presentation]

None

[Others (Book, Press release, etc.)]

None